A THESIS

FOR THE DEGREE OF MASTER OF SCIENCE

Aqueous Extract of Freeze Dried *Protaetia brevitarsis* Larvae-Induced Immunostimulation and Bone Formation

Jayasingha Arachchige Chathuranga Chanaka Jayasingha

Department of Marine Life Science

GRADUATE SCHOOL

JEJU NATIONAL UNIVERSITY

FREBUARY, 2022

Aqueous Extract of Freeze Dried *Protaetia brevitarsis* Larvae-Induced Immunostimulation and Bone Formation

Jayasingha Arachchige Chathuranga Chanaka Jayasingha

(Supervised by Professor Gi-Young Kim)

A thesis submitted in partial fulfillment of the requirement for the degree of masters

December 2021

The thesis has been examined and approved by

.....

Woong Han, Principal Researcher of Nakdonggang National Institute of Biological Resources

.....

Gi-Young Kim, Professor of Jeju National University

.....

Chang-Hee Kang, Senior Researcher of Nakdonggang National Institute of Biological Resources

02.12.2020

Date

Department of Marine Life Science

GRADUATE SCHOOL

JEJU NATIONAL UNIVERSITY

CONTENTS

List of Figures

Acknowledgement

My deep gratitude firstly goes to Professor Kim Gi-Young for supporting me to complete the first step of my research journey. Without Professor Kim Gi-Young's guidance thesis would not be a reality and i would highly appreciate professor's commitment and curiosity in research work, which were high motivation factors for me to complete my thesis work. I respect his attitude and research sense, which are really assets to me as a student.

At the same moment i need to express my thanks and gratitude to my lab members, who were behind me every time in my experiments. My special thank goes to Mr. Hasitha Karunarathne for their limitless support towards me continuously, even though they were busy with their research work.

I would like to take this opportunity to former lab members Dr. Neelaka Molagoda and Dr. Prasad Jayasooriya, who indicated he successful outcome of the research work and by their continuous commitment. Specially, Dr. Neelaka every time encouraged me through this journey.

Next, i would like to thank my undergraduate supervisor Senior Professor Ariya Sumanasinghe, who encouraged for the higher studies. I should express my gratitude to all the teachers, who supported me, including my advanced level Biology teacher Mrs. Janitha.

Finally, i need to thank the most important part of my life, my parents, Mrs. Swarna Armour Perera and Mr. Sisil Jayasinghe and brother, Mr. Buddhika Jayasinghe, who were roots for my education every time and without them i am not here to do this research work. I would honestly express my gratitude towards them for waiting for my successful future and career at the same time, i need to thank Bimali, who is waiting for my successful future.

Summary

White-spotted flower chafer (*Protaetia brevitarsis*) larvae are a potential nutritional supplement and have been used in traditional Asian herbal medicine with plenty of nutrients and minerals and possess neuroprotective and antioxidative activity. In the first phase of this study, we found that aqueous extract of freeze-dried *P. brevitarsis* larvae (AEPB) promotes immunostimulation in RAW 264.7 macrophages. No significant cytotoxicity was observed below 800 μg/mL AEPB. Moreover, AEPB treatment enhanced the production of nitric oxide (NO), prostaglandin E_2 (PGE_2), interleukin (IL)-6, and IL-12 through the upregulation of their regulatory genes. AEPB also promoted the nuclear translocation of nuclear factor-κB (NF-κB), and pyrrolidine dithiocarbamate, an inhibitor of NF-κB activation, remarkably prevented the expression of AEPB-induced *inducible NO synthase* (*iNOS*), *cyclooxygenase-2* (*COX-2*), *IL-6*, and *IL-12*, indicating that AEPB promotes the production of immunostimulants such as NO and PGE_2 and pro-inflammatory cytokines such as IL-6 and IL-12 in RAW 264.7 macrophages by activating the NF-κB signaling pathway. Moreover, AEPB upregulated the extracellular expression of Toll-like receptor 4 (TLR4) and subsequently increased myeloid differentiation primary response 88 (MyD88) and IL-1 receptor-associated kinase 4 (IRAK4) expression, which indicates that AEPB activated the NF-κB signaling pathway through the TLR4-mediated MyD88 and IRAK4 axis. Collectively, this study provides evidence that AEPB is a promising nutritional supplement for stimulating macrophage-mediated immune responses.

In the second phase of the study, we targeted whether AEPB could act on osteoblast differentiation in pre-osteoblast MC3T3-E1 cells, since AEPB has not been identified in osteoblast differentiation. Next, we found that AEPB highly promotes expression of osteogenic genes including runt-related transcription factor 2 (RUNX2), osterix (OSX), and alkaline

phosphatase (ALP) along with high level of mineralization in preosteoblast MC3T3-E1 cells. Moreover, AEPB accelerated vertebral formation in zebrafish larvae accompanied by the osteogenic gene expression. Inhibition of the Wnt/β-catenin signaling pathway using FH535 suppressed AEPB-induced osteogenic gene expression and vertebral formation, which indicates that AEPB stimulated osteogenesis by activating the Wnt/β-catenin signaling pathway. Taken together, this study confirms that AEPB is a promising supplement for osteoblast differentiation and bone formation. Nevertheless, whether AEPB inhibits bone resorption diseases such as osteoporosis should be evaluated in higher animal models.

논문 요약

흰 반점 꽃 풍뎅이과(Protaetia brevitarsis) 유충은 잠재적인 영양 보충제이며 영양과 미네랄이 풍부하고 신경 보호 및 항산화 활성을 가지고 있어 전통 아시아 약초에서 사용되었습니다. 이 연구의 첫 번째 단계에서 우리는 동결 건조된 P. brevitarsis 유충(AEPB)의 수성 추출물이 RAW 264.7 대식세포에서 면역 자극을 촉진한다는 것을 발견했습니다. 800 μg/mL AEPB 미만에서는 유의한 세포독성이 관찰되지 않았다. 또한, AEPB 처리는 조절 유전자의 상향 조절을 통해 산화질소(NO), 프로스타글란딘 E2(PGE2), 인터루킨(IL)-6 및 IL-12 의 생성을 향상시켰습니다. AEPB 는 또한 핵인자-κB(NF-κB)의 핵전위를 촉진시켰고, NF-κB 활성화 억제제인 pyrrolidine dithiocarbamate 는 AEPB 에 의해 유도되는 iNOS(inducible NO synthase), cyclooxygenase-2(COX- 2), IL-6 및 IL-12, 이는 AEPB 가 NF-κB 신호전달을 활성화함으로써 RAW 264.7 대식세포에서 NO 및 PGE2 와 같은 면역자극제와 IL-6 및 IL-12 와 같은 전염증성 사이토카인의 생성을 촉진함을 나타냅니다. 좁은 길. 더욱이, AEPB 는 Toll-유사 수용체 4(TLR4)의 세포외 발현을 상향조절하고, 이어서 골수 분화 1 차 반응 88(MyD88) 및 IL-1 수용체 관련 키나제 4(IRAK4) 발현을 증가시켰으며, 이는 AEPB 가 NF-κB 를 활성화했음을 나타냅니다. TLR4 매개 MyD88 및 IRAK4 축을 통한 신호 전달 경로. 종합적으로, 이 연구는 AEPB 가 대식세포 매개 면역 반응을 자극하기 위한 유망한 영양 보충제라는 증거를 제공합니다.

연구의 두 번째 단계에서 우리는 AEPB 가 조골 세포 분화에서 확인되지 않았기 때문에 AEPB 가 전 조골 세포 MC3T3-E1 세포에서 조골 세포 분화에 작용할 수 있는지 여부를 목표로 삼았습니다. 다음으로, 우리는 AEPB 가 골아세포 MC3T3-E1 세포에서 높은 수준의 광물화와 함께 런트 관련 전사 인자 2(RUNX2), 오스테릭스(OSX) 및 알칼리성 포스파타제(ALP)를 포함한 골형성 유전자의 발현을 고도로 촉진한다는 것을 발견했습니다. 더욱이, AEPB 는 골형성 유전자 발현을 수반하는 제브라피쉬 유충의 척추 형성을 가속화했습니다. FH535 를 이용한 Wnt/β-카테닌 신호전달 경로의 억제는 AEPB 에 의한 골형성 유전자 발현과 척추 형성을 억제했는데, 이는 AEPB 가 Wnt/β-카테닌 신호전달 경로를 활성화시켜 골형성을 자극했음을 시사한다. 종합하면, 이 연구는 AEPB 가 조골세포 분화 및 뼈 형성을 위한 유망한 보충제임을 확인합니다. 그럼에도 불구하고, AEPB 가 골다공증과 같은 골흡수 질환을 억제하는지 여부는 고등 동물 모델에서 평가되어야 한다.

Chapter 1

An aqueous extract of freeze-dried *Protaetia brevitarsis* larvae enhances immunostimulatory activity in RAW 264.7 macrophages by activating the NF-κB signaling pathway

Abstract

White-spotted flower chafer (*Protaetia brevitarsis*) larvae are a potential nutritional supplement and have been used in traditional Asian herbal medicine. In this study, we found that an aqueous extract of freeze-dried *P. brevitarsis* larvae (AEPB) promotes immunostimulation in RAW 264.7 macrophages. No significant cytotoxicity was observed below 800 μg/mL AEPB. Moreover, AEPB treatment enhanced the production of nitric oxide (NO), prostaglandin E_2 (PGE_2), interleukin (IL)-6, and IL-12 through the upregulation of their regulatory genes. AEPB also promoted the nuclear translocation of nuclear factor-κB (NF-κB), and pyrrolidine dithiocarbamate, an inhibitor of NF-κB activation, remarkably prevented the expression of AEPB-induced *inducible NO synthase* (*iNOS*), *cyclooxygenase-2* (*COX-2*), *IL-6*, and *IL-12*, indicating that AEPB promotes the production of immunostimulants such as NO and PGE_2 and pro-inflammatory cytokines such as IL-6 and IL-12 in RAW 264.7 macrophages by activating the NF-κB signaling pathway. Moreover, AEPB upregulated the extracellular expression of Toll-like receptor 4 (TLR4) and subsequently increased myeloid differentiation primary response 88 (MyD88) and IL-1 receptor-associated kinase 4 (IRAK4) expression, which indicates that AEPB activated the NF-κB signaling pathway through the TLR4-mediated MyD88 and IRAK4 axis. Collectively, this study provides evidence that AEPB is a promising nutritional supplement for stimulating macrophage-mediated immune responses.

Keywords: *Protaetia brevitarsis*; nuclear factor-κB; Toll-like receptor 4; Immunostimulation

Practical Application: An aqueous extract of *P. brevitarsis* stimulates immune responses in RAW 264.7 macrophages

1.1 Introduction

The innate immune system in vertebrates is mediated by phagocytes such as macrophages and neutrophils, which eliminate pathogens such as bacteria and viruses, and trigger the adaptive immune system to generate immune memory against invading pathogens (Riera Romo, Perez-Martinez, & Castillo Ferrer, 2016). Macrophages play an essential role in immunomodulation against infections and tumors by producing immunostimulants such as nitric oxide (NO) and prostaglandin E_2 (PGE_2), and pro-inflammatory cytokines such as interleukin (IL)-6, and IL-12 (Chaplin, 2010; Locati, Mantovani, & Sica, 2013). Nuclear factor-κB (NF-κB) is a well-known transcription factor that regulates the expression of immunostimulant genes such as *inducible NO synthase* (*iNOS*) and *cyclooxygenase-2* (*COX-2*), pro-inflammatory cytokines such as *IL-6*, and *IL-12* (Liu, Zhang, Joo, & Sun, 2017). Upon stimulation via numerous immunoregulating receptors such as Toll-like receptors (TLRs), NF-κB is released from the IκB complex, and, in turn, is translocated to the nucleus, which enhances the transcription of immunostimulant and pro-inflammatory cytokine genes by binding to the promoter regions of the target genes (Liu et al., 2017). Therefore, natural and synthetic agents that can enhance NF-κB activation, boost early defense mechanisms and increase resistance against infectious pathogens (Rahman & McFadden, 2011).

Approximately 2,000 species of insects have been used as dietary supplements due to their abundant nutrients compared with other meat sources (Yoon et al., 2020). In particular, *Protaetia brevitarsis* larvae are considered, in Korean traditional medicine, as a promising nutritional source for the treatment of many human disorders including stomatitis, tetanus, hepatic cancer, liver cirrhosis, and cerebral stroke (Lee et al., 2017). Recent reports showed that freeze-dried *P. brevitarsis* larva power contained 58% crude protein, 17% crude fat, and 11% total carbohydrate with crude ash and fiber, and showed no evidence of mutagenic and

carcinogenic potential in a genotoxicity study (Noh et al., 2018; Yoon et al., 2020). In addition, *P. brevitarsis* larva extract possessed antioxidant and anti-cancer activities (Suh & Kang, 2012; Yoo et al., 2007). Nevertheless, whether *P. brevitarsis* extract regulates the innate immune system remains unclear.

In this study, we investigated whether an aqueous extract of *P. brevitarsis* larvae (AEPB) stimulates immune responses in RAW 264.7 macrophages. We found that AEPB increased the production of NO, PGE_2, IL-6, and IL-12 via increased expression of their regulatory genes such as *inducible* NO *synthase* (*iNOS*), *cyclooxygenase-2* (*COX-2*), *IL-6*, and *IL-12*. In addition, AEPB upregulated the expression of TLR4 on the membranes of RAW 264.7 macrophages, which activates MyD88 and IRAK4, and subsequently stimulates NF-κB. Collectively, these data indicate that AEPB can be used as an immunostimulant nutritional supplement to activate macrophages.

1.2 Materials and methods

1.2.1 Reagents and antibodies

Pyrrolidine dithiocarbamate (PDTC), lipopolysaccharides (LPS from *Escherichia coli* O55:B5), 3-(4,5-dimethylthiazol-2-yl)-2,5-diphenyltetrazolium bromide (MTT), and 4′,6-diamidine-2-phenylindole dihydrochloride (DAPI) were purchased from Sigma-Aldrich (St. Louis, MO, USA). Antibodies against iNOS (sc-7221), COX-2 (sc-8414), β-actin (sc-69879), p50 (sc-8414), p65 (sc-8008), nucleolin (sc-13057), and TLR4 (sc-293072) were purchased from Santa Cruz Biotechnology (Santa Cruz, CA, USA). Antibody against MyD88 (GTX112987) and phospho (p)-IRAK-4 (Thr345/Ser346, #7652) were purchased from GeneTex (Irvine, CA, USA) and Cell Signaling Technology (Beverly, MA, USA), respectively. Secondary antibodies conjugated with Alex Fluor® 488 and Alex Fluor® 647 were obtained

from Abcam (Cambridge, MA, UK). Dulbecco's Modified Eagle's Medium (DMEM), fetal bovine serum (FBS), and antibiotic mixtures were purchased from WelGENE Inc. (Daegu, Republic of Korea). Peroxidase-labeled anti-rabbit and anti-mouse immunoglobulins were obtained from KOMA BIOTECH (Seoul, Republic of Korea). Other all the chemicals were purchased from Sigma-Aldrich.

1.2.2 Cell culture and cell viability assay

RAW 264.7 macrophages were cultured in DMEM supplemented with 5% FBS and antibiotic mixtures at 37℃ in a humidified incubator with 5% CO_2. Relative cell viability was measured by an MTT assay. In brief, the cells were seeded at a density of 1×10^5 cells/mL and treated with the indicated concentrations of AEPB (0–800 μg/mL). LPS (500 ng/mL) was used as a positive control. After treatment with AEPB and LPS for 24 h, MTT solution (0.5 mg/mL) was added to each well and incubated for 30 min at 37℃. The medium was discarded and crystal formazan was dissolved by dimethyl sulfoxide. Absorbance was measured at a wavelength of 540 nm using an ELISA microplate reader (BioTek Instruments Inc., Winooski, VT, USA). In a parallel experiment, cell morphology was observed using a phase-contrast microscope (Ezscope i900PH, MACROTECH, Goyang, Gyeonggido, Republic of Korea).

1.2.3 NO assay

NO production was measured by Griess reagent assay. Briefly, RAW 264.7 macrophages were seeded at a density of 1×10^5 cells/mL and treated with the indicated concentrations AEPB (0–800 μg/mL) and 500 ng/mL LPS for 24 h. Culture media were collected and mixed with the same volume of Griess reagent (1% sulfanilamide in 5% phosphoric acid and 0.1% naphthylethylenediamine dihydrochloride) for 15 min. Absorbance was measured at the wavelength of 590 nm using an ELISA plate reader (BioTek Instruments Inc.). NO

concentrations were calculated from a standard curve of sodium nitrite ($NaNO_2$) and fresh medium was used as a blank control.

1.2.4 Enzyme-linked immunosorbent assay (ELISA)

ELISA was performed to quantify the secreted levels of PGE_2 (Cayman Chemicals, Ann Arbor, MI, USA), IL-6 (R&D Systems, Minneapolis, MN, USA), and IL-12 (R&D Systems). Briefly, RAW 264.7 macrophages were seeded at a density 1×10^5 cells/mL and treated with the indicated concentrations of AEPB (0–800 μg/mL) and LPS (500 ng/mL) for 48 h. The cell culture supernatants were collected and the concentrations of PGE_2, IL-6, and IL-12 were determined at a wavelength of 450 nm using an ELISA plate reader (BioTek Instruments Inc.).

1.2.5 Isolation of total RNA from RAW 264.7 macrophage and RT-PCR

Total RNA was isolated from RAW 264.7 macrophages using an easy-BLUE^{TM} total RNA extraction kit (iNtRON Biotechnology, Seongnam, Gyeonggido, Republic of Korea). Reverse transcription was performed by Moloney murine leukemia virus reverse transcriptase (MMLV) (BIONEER, Daejeon, Republic of Korea) and synthesized cDNAs were used to amplify the target genes using specific primers (Molagoda et al., 2019): *iNOS* (199 bp) sense 5′-CCT CCT CCA CCC TAC CAA GT-3′ and anti-sense 5′-CAC CCA AAG TGC TTC AGT CA-3′; *COX-2* (141 bp) sense 5′-TGC TGT ACC AGC AGT GGC AA-3′ and anti-sense 5′-GCA GCC ATT TCC TTC TCT CC-3′; *IL-6* (141 bp) sense 5′-AAG TGC ATC ATC GTT GTT TTC A-3′ and anti-sense 5′-GAG GAT ACC ACT CCC AAC AG-3′; *IL-12 p35* (334 bp) sense 5′-TCT AAC TTC AGC GCA GTG GA-3′ and anti-sense 5′- TGC GGT GGT GTA GTG AGT G-3′; and *GAPDH* (123 bp) sense 5′- AGG TCG GTG TGA ACG GAT TTG-3′ and anti-sense 5′-TGT AGA CCA TGT AGT TGA GGT CA-3′. *iNOS*, *IL-12 p35*, *IL-6* and *GAPDH* were amplified by 25 cycles of denaturation at 95℃ for 30 s, annealing at 55℃ for 30 s, and extended at 72℃

for 30 s. *COX-2* was amplified by 32 cycles of denaturation at 95°C for 30 s, annealing at 57°C for 30 s, and extended at 72°C for 30 s. *GAPDH* was used as an internal control to evaluate relative expression of *iNOS*, *COX-2*, *IL-6*, and *IL-12*.

1.2.6 Western blotting

Total protein was extracted using RIPA lysis buffer (iNtRON Biotechnology). In brief, RAW 264.7 macrophages were lysed with the lysis buffer for 30 min, and lysates were centrifuged at 14,000× *g* at 4℃ for 10 min. In a parallel experiment, nuclear and cytoplasmic proteins were separately isolated using NE-PER nuclear and cytosolic extraction reagents (Pierce, Rockford, IL, USA). Protein concentrations of the lysates were determined using a Bio-Rad protein assay kit (Bio-Rad, Hercules, CA, USA). Then, western blotting was performed on 10% SDS-polyacrylamide gel electrophoresis (SDS-PAGE) and the proteins were transferred to the polyvinylidene difluoride membrane. After blocking the membrane with 5% non-fat dry milk in phosphate-buffered saline with 0.1% Tween-20 (PBST), the membranes were incubated with the indicated primary (200 μg/mL, 1:1,000 dilution) and secondary antibodies (400 μg/mL, 1:10,000 dilution), respectively. Finally, the expression of each protein was monitored using an enhanced chemiluminescence detection system (Pierce).

1.2.7 Immunofluorescence staining of p65 and TLR4

RAW 264.7 macrophages were seeded at a density of 1×10^4 cells/mL on 3% gelatin-coated coverslips. AEPB (0–800 μg/mL) was treated for 1 h and fixed with 4% paraformaldehyde for 10 min at 37℃. The fixed cells were permeabilized with 0.1% Triton X-100 for 10 min at room temperature. The cells were washed with ice-cold PBST for 5 min, blocked with 10% donkey serum for 1 h, and then incubated with p65 and TLR4 antibodies (200 μg/ml, 1:100 dilutions in 10% donkey serum) at 4℃ overnight. The cells were washed

with ice-cold PBST and incubated with secondary antibodies conjugated Alexa Fluor® 647 (for p65) and Alexa Fluor® 488 (for TLR4) for 2 h at room temperature. Finally, the cells were counterstained with nuclear staining dye, DAPI (300 nM), for 10 min. The coverslips were mounted onto glass slides using aqueous mounting media (DAKO, Carpinteria, CA, USA). Finally, the fluorescence images were detected by a CELENA® S digital imaging system (Logos Biosystems, Anyang, Gyeonggido, Republic of Korea).

1.2.8 Statistical analysis

All experiments were performed in triplicate. The images of RT-PCR and western blotting were visualized by ImageQuant LAS 500 (GE Healthcare Bio-Sciences AB, Uppsala, Sweden) and transported into Adobe Photoshop. Statistical analysis was performed and graphed using Sigma Plot 12.0 software by unpaired one-way analysis of variance (ANOVA) with Bonferroni correction. All data were expressed as the mean ± the standard error of the median (SEM). Statistical significance was set at *, $p < 0.001$.

1.3 Results

1.3.1 No evidence of cytotoxic potential is observed in AEPB-treated RAW 264.7 macrophages

To investigate whether AEPB influences cytotoxicity, RAW 264.7 macrophages were treated with various concentrations of AEPB for 24 h, and morphological changes and relative cell viability were measured. Morphological death was not observed in AEPB-treated RAW 264.7 macrophages. Untreated cells and those treated with low concentrations of AEPB (≤ 200 μg/mL) showed rounded cell morphology. In contrast, high concentrations of AEPB (≥ 400 μg/mL) induced marked formation of cytoplasmic projections or extended pseudopodia (Figure 1A), which indicated that high concentrations of AEPB phenotypically activated RAW 264.7

macrophages. In addition, no significant changes in relative cell viability were observed at any concentration of AEPB tested in this study (Figure 1B). These data indicate that AEPB possesses no direct cytotoxicity and triggers phenotypical activation in RAW 264.7 macrophages.

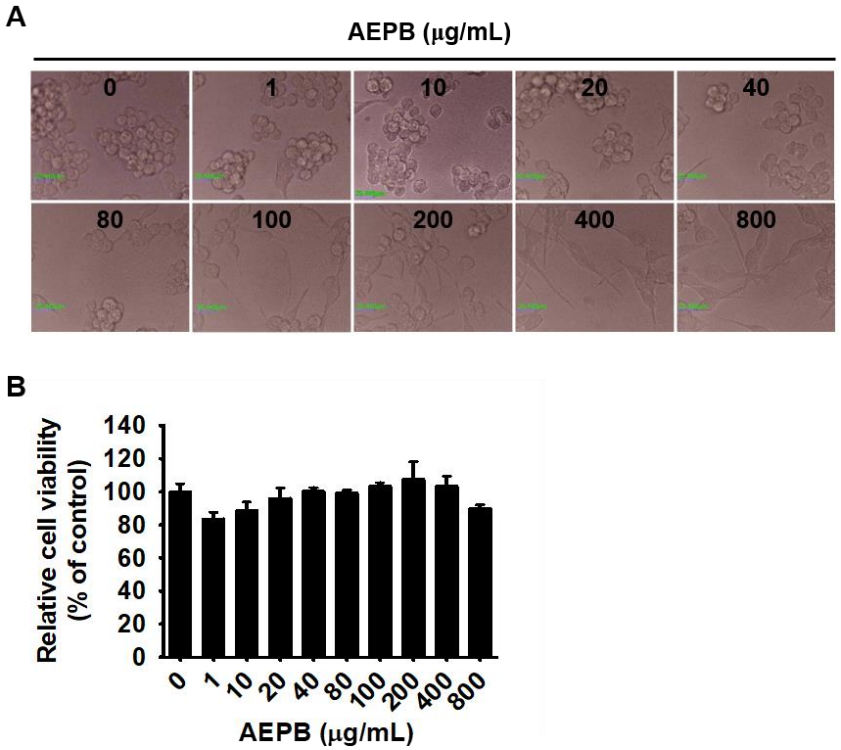

Figure 1.AEPB triggers phenotypical activation in RAW 264.7 macrophages without any cytotoxicity

RAW 264.7 macrophages were seeded at a density of 1×10^5 cells/mL and treated with the indicated concentrations of AEPB (0–800 μg/mL) for 24 h. (A) Images of RAW 264.7 macrophages were captured using a phase-contrast microscope. Scale bar = 20 μm. (B) An MTT assay was used to determine relative cell viability. Data are presented as the mean ± SEM.

1.3.2 AEPB induces the expression of iNOS and COX-2 in RAW 264.7 macrophages and, in turn, increased the secreted levels of NO and PGE_2

We investigated whether AEPB induces the production of NO and PGE_2 accompanied by

specific regulatory genes such as *iNOS* and *COX-2*. AEPB-treated RAW 264.7 macrophages increased the expression of iNOS mRNA at 9 h (Figure 2A) and protein at 24 h (Figure 2B) in a concentration-dependent manner. The highest concentration of AEPB markedly enhanced the expression of iNOS, which was comparable to that observed in LPS-treated cells. Consistent with the data regarding the expression of iNOS, AEPB at 400 and 800 μg/mL significantly increased the expression of COX-2 mRNA at 9 h (Figure 2C) and protein at 24 h (Figure 2D). In addition, AEPB significantly increased NO production at high concentrations (14.4 ± 1.5 μM and 20.4 ± 2.0 μM at 400 and 800 μg/mL, respectively), which was comparable to the amount of NO from LPS-treated cells (19.4 ± 1.5 μM). However, no treatment or a low concentration of AEPB (100 μg/mL) induced no significant NO production in RAW 264.7 macrophages (Figure 2E). Furthermore, AEPB significantly enhanced the production of PGE_2 at 800 μg/mL (2345.0 ± 67.2 pg/mL), comparable to that observed in LPS-treated cells (2318.6 ± 87.1 pg/mL, Figure 2F). AEPB at 400 μg/mL moderately increased the release of PGE_2 (883.3 ± 96.9 pg/mL), but the low concentration of AEPB (100 μg/mL) did not enhance the production of PGE_2 (234.8 ± 35.6 pg/mL). These data indicate that AEPB increases the production of NO and PGE_2 accompanied by the high expression of their regulatory genes, such as *iNOS* and *COX-2*.

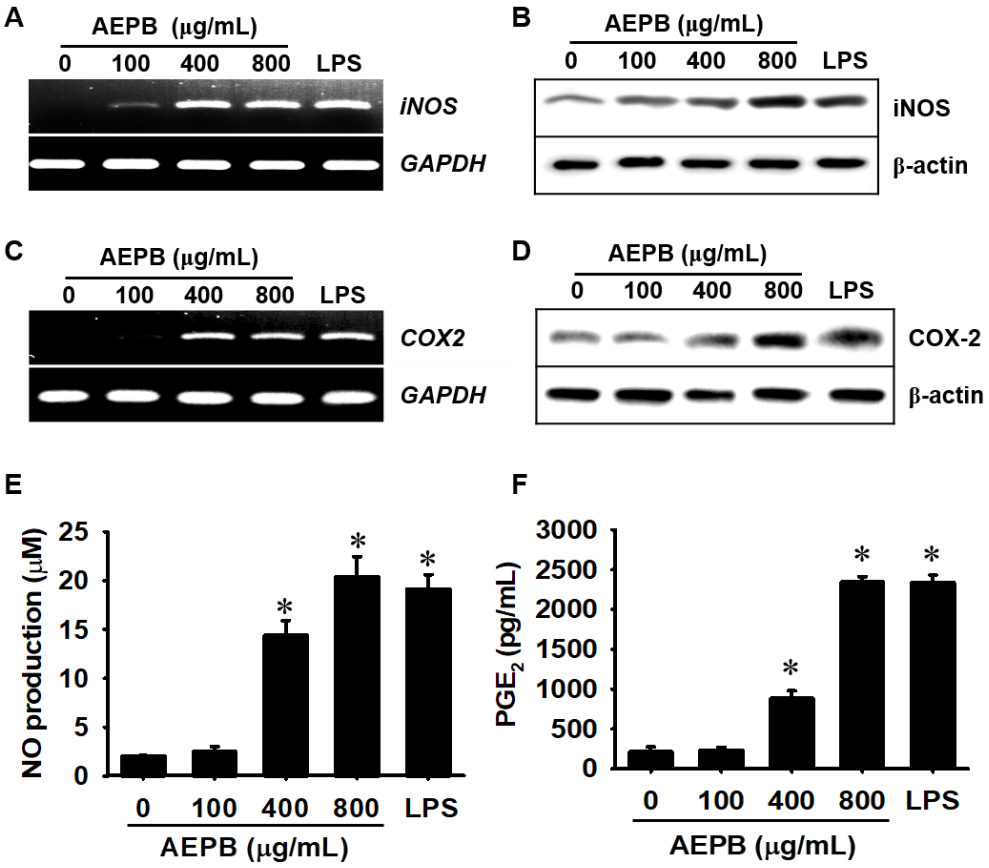

Figure 2. AEPB treatment enhances the expression of iNOS and COX-2 in RAW 264.7 macrophages, increasing no and PGE2.

RAW 264.7 macrophages were seeded at a density of 1 × 10^5 cells/mL and then treated with the indicated concentrations of AEPB (0–800 μg/mL) and 500 ng/mL LPS. (A and C) Total RNA was extracted at 9 h and RT-PCR was performed to measure the expression of (A) *iNOS* and (C) *COX-2*. *GAPDH* was used as an internal control. (B and D) Total protein was extracted at 24 h and then, western blotting was performed to detect the expressed levels of (B) iNOS and (D) COX-2. β-Actin was used as an internal control. (E-F) In a parallel experiment, the cells were treated with AEPB. (E) NO production was detected using a Griess reagent assay at 24 h. (D) The extracellular release of PGE_2 was measured using a PGE_2 ELISA kit at 48 h. Data are presented as the mean ± SEM. The statistical significance was determined by one-way ANOVA (* $p < 0.001$ *vs*. untreated cells).

1.3.3 AEPB induces the expression and secretion of pro-inflammatory cytokines such as IL-6 and IL-12 in RAW 264.7 macrophages

We also investigated whether AEPB enhances the expression of pro-inflammatory cytokines such as IL-6 and IL-12. AEPB at 800 μg/mL markedly upregulated the expression of both *IL-6* (Figure 3A) and *IL-12* (Figure 3B) at 9 h, which were significantly greater than that seen with 400 μg/mL. Consistent with RT-PCR data, IL-6 production increased in response to AEPB in RAW 264.7 macrophages (135.4 ± 0.8 pg/mL and 164.3 ± 5.7 pg/mL at 400 and 800 μg/mL AEPB, respectively), and the levels were comparable to those in LPS-treated cells (161.8 ± 5.1 pg/mL). However, the untreated cells showed low levels of IL-6 production (45.3 ± 2.3 pg/mL), which was similar to treatment with 100 μg/mL AEPB (49.584 ± 2.612 pg/mL) (Figure 3C). IL-12 production also significantly increased to 882.6 ± 142.9 pg/mL and 1197.4 ± 77.3 pg/mL at 400 and 800 μg/mL AEPB, respectively, which was comparable to that observed in LPS-treated cells (1153.0 ± 31.6 pg/mL) (Figure 3D). Consistent with the data regarding IL-6 production, the untreated cells and 100 μg/mL AEPB released low levels of IL-12 (164.1 ± 45.1 pg/mL and 171.5 ± 63.3 pg/mL, respectively). These data indicate that AEPB stimulates the expression of cytokine genes such as *IL-6* and *IL-12*, resulting in increased IL-6 and IL-12 release.

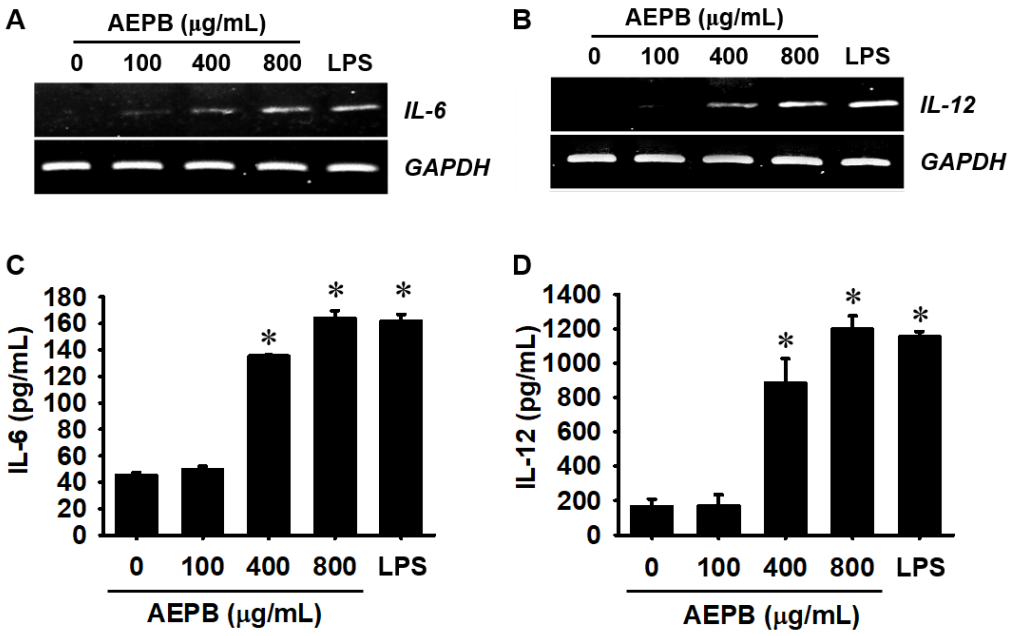

Figure 3. AEPB stimulates the expression of *IL-6* and *IL-12* and increases the release of IL-6 and IL-12.

RAW 264.7 macrophages were seeded at a density of 1×10^5 cells/mL and then treated with the indicated concentrations of AEPB (0–800 μg/mL). (A-B) Total RNA was extracted at 9 h and then RT-PCR was performed to detect the expression of (A) *IL-6* and (B) *IL-12*. *GAPDH* was used as an internal control. (C-D) After treatment with AEPB and LPS for 48 h, ELISA was performed to measure the extracellular release of (C) IL-6 and (D) IL-12. Data are presented as the mean ± SEM. The statistical significance was determined using one-way ANOVA (* $p < 0.001$ *vs*. untreated cells).

1.3.4 AEPB activates nuclear translocation of NF-κB, resulting in the expression of immunostimulant genes

Since the NF-κB pathway is the key to transactivating the expression of immunostimulants and pro-inflammatory cytokines (Liu et al., 2017; Rahman & McFadden, 2011), we investigated whether AEPB activates the NF-κB signaling pathway. Immunofluorescence

staining showed that the highest concentration of AEPB (800 μg/mL) remarkably promoted the nuclear translocation of the NF-κB subunit p65, which was similar to that observed in LPS-treated cells. Furthermore, 400 μg/mL AEPB moderately stimulated the translocation of p65 to the nucleus; however, no discrete nuclear translocation of p65 was observed below 100 μg/mL AEPB (Figure 4A). In addition, western blot analysis revealed that AEPB increased the high levels of NF-κB subunits such as p65 and p50 in the nucleus, which indicates that AEPB activates NF-κB (Figure 4B). To confirm the function of AEPB-induced NF-κB translocation, RAW 264.7 macrophages were pretreated with PDTC, an NF-κB inhibitor, and the expression of immunostimulant and pro-inflammatory cytokines genes were measured. Pretreatment with PDTC resulted in a significant reduction of both AEPB- and LPS-induced immunostimulant and pro-inflammatory cytokine gene expression, which indicates that AEPB stimulates nuclear translocation and subsequent activation of NF-κB, as well as the increased expression of immunostimulant and pro-inflammatory cytokine genes.

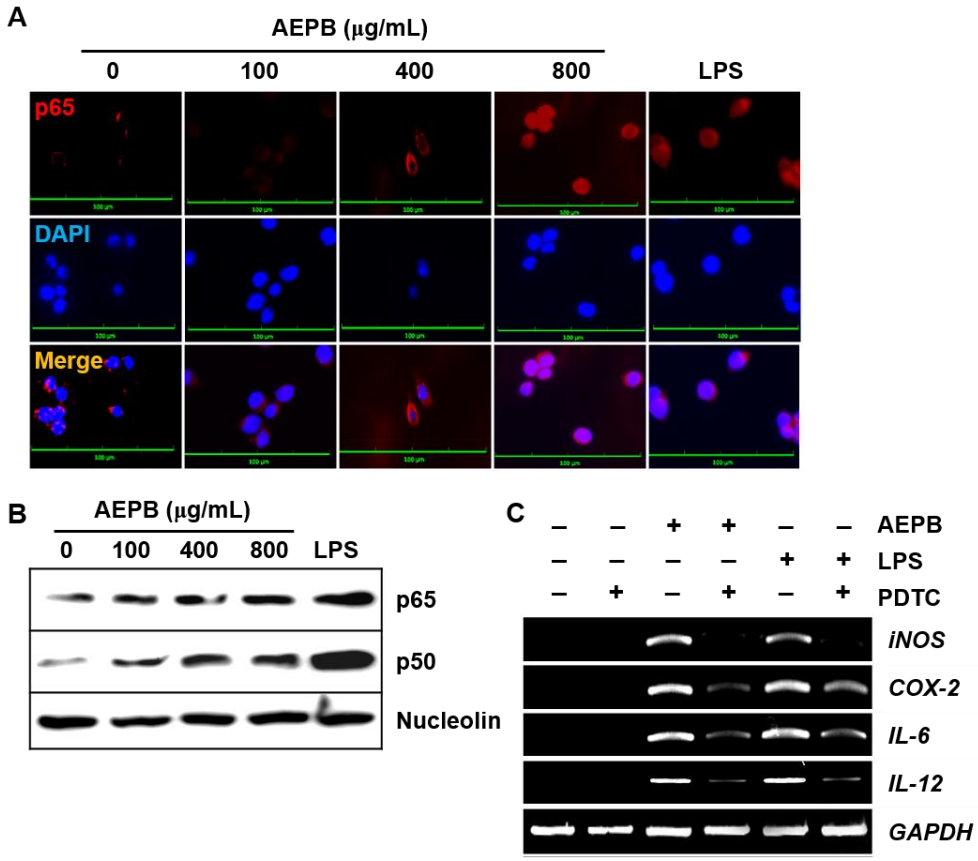

Figure 4. AEPB promotes nuclear translocation of NF-KB and, in turn, stimulates the expression of pro-inflammatory cytokine genes.

RAW 264.7 macrophages were treated with the indicated concentrations of AEPB (0–800 μg/mL) and 500 ng/mL LPS. (A) After treatment for 2 h, NF-κB p65 was immunostained with an anti-p65 antibody and detected using a secondary antibody conjugated with Alex Fluor® 647, followed by nuclear counterstaining with DAPI. The fluorescence was analyzed using a CELENA® S digital imaging system. Scale bar = 100 μm. (B) The nuclear expression of NF-κB p50 and p65 was detected 30 min after treatment with AEPB. Nucleolin was used as an internal control. (C) RAW 264.7 macrophages were pretreated with 10 μM PDTC for 2 h and then treated with 800 μg/mL AEPB and 500 ng/mL LPS for 9 h. Total RNA was extracted and RT-PCR was performed. *GAPDH* was used as an internal control. LPS (500 ng/mL) was used as a positive control.

1.3.5 AEPB stimulates the TLR4-mediated signaling pathway in RAW 264.7 macrophages

TLR4 is a pattern recognition receptor that stimulates the expression of immunostimulant and pro-inflammatory cytokine genes by activating the NF-κB signaling pathway via MyD88 and IRAK4 (Dorrington & Fraser, 2019). Therefore, we investigated whether AEPB influences the TLR4-mediated signaling pathway. As shown in Figure 5A, AEPB intensified the TLR4 fluorescence on membranes of RAW 264.7 macrophages in a concentration-dependent manner. In addition, the expression of MyD88 and phosphorylation of IRAK-4 were upregulated in response to AEPB treatment; 800 μg/mL AEPB significantly increased expression similar to levels induced by LPS. Likewise, 400 μg/mL AEPB treatment produced a moderate increase (Figure 5B). These data indicate that AEPB can activate TLR4-mediated MyD88 and IRAK4.

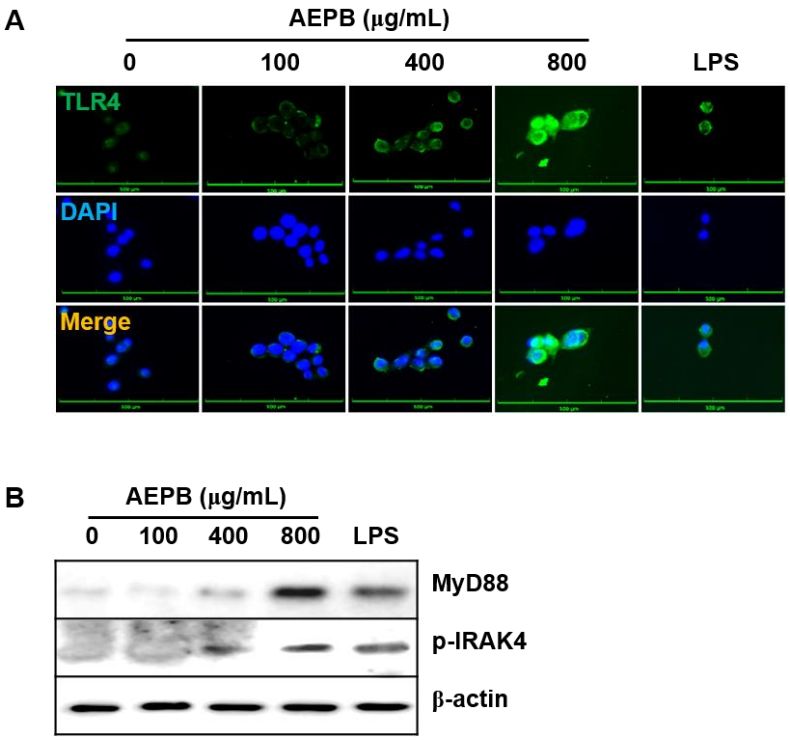

Figure 5. AEPB stimulates TLR4-mediated activation of MYD88 and IRAK4

RAW 264.7 macrophages were treated with the indicated concentrations of AEPB (0–800 μg/mL) and 500 ng/mL LPS. (A) After treatment for 3 h, the TLR4 present on cell membranes

was immunostained with an anti-TLR4 antibody (Ab), and secondary Ab conjugated with Alexa Fluor® 488 followed by nuclear counterstaining with DAPI. The fluorescence was analyzed using a CELENA® S digital imaging system. (B) In a parallel experiment, total protein was extracted at 30 min, and western blotting was performed.

1.4 Discussion

P. brevitarsis is an edible insect that contains abundant nutrients with no genotoxicity (Noh et al., 2018; Yoon et al., 2020). Recently, some studies have shown that *P. brevitarsis* extract possessed anti-obesity (Ahn, Myung, Jung, & Kim, 2019), antioxidant (Suh & Kang, 2012), anti-cancer (Yoo et al., 2007), and hepatoprotective properties (Im, Yang, Park, Kim, & Chae, 2018). Nevertheless, whether *P. brevitarsis* extract influences innate immune responses remains unclear. In this study, we found that AEPB enhances the release of immunostimulants such as NO and PGE_2, and pro-inflammatory cytokines such as IL-6 and IL-12, accompanied by the increased expression of their regulatory genes through the activation of the TLR4-mediated NF-κB signaling pathway. These data show that AEPB may be a potential immunostimulant supplement.

During the early stages of an invasion by pathogens such as bacteria, macrophages play an essential role in host innate immune responses through the massive production of immunostimulants and pro-inflammatory cytokines concomitant with phagocytosis, which removes extracellular pathogens (Hirayama, Iida, & Nakase, 2017). In addition, macrophages contribute to the activation of adaptive immune responses through the engulfment and digestion of pathogens through the expression of MHCII and co-stimulatory molecules such as CD80 and CD86 (Iwasaki & Medzhitov, 2015). Macrophages recognize specific molecular patterns derived from invasive pathogens using pattern recognition receptors such as TLRs,

which in turn activate immune systems (Billack, 2006; Grassin-Delyle et al., 2020). In particular, TLR4 is known to recognize LPS from gram-negative bacteria, polysaccharides, viral proteins, and endogenous proteins such as low-density proteins and heat shock proteins (Brubaker, Bonham, Zanoni, & Kagan, 2015). When specific agonists bind to TLR4 with MD2, MyD88 and IRAK4 are recruited in the intracellular Toll/IL-1 receptor (TIR) domain of TLR4. This recruitment canonically stimulates the activation of NF-κB, which enhances the expression of immunostimulants and pro-inflammatory cytokines (Liu et al., 2017). In this regard, many herbal medicines such as polysaccharides target the TLR4 signaling pathway to boost innate and adaptive immune responses *in vitro* and *in vivo*, which produces the promising potential as vaccine adjuvants (Gao, Zhou, Jiang, Huang, & Dai, 2003; Li et al., 2015; Zhang, Qi, Guo, Zhou, & Zhang, 2016). In addition, natural and synthetic TLR agonists have been considered as vaccine adjuvants for increasing innate defense mechanisms against invasive pathogens and cancers (Feng et al., 2019; Ireton & Reed, 2013; Johnson, 2013). In this study, we found that AEPB increased the expression of immunostimulants and pro-inflammatory cytokines by activating the TLR4-mediated NF-κB signaling pathway, which suggests that AEPB is a promising nutritional supplement for boosting the innate immune system. Nevertheless, further experiments are needed to evaluate which components of AEPB are effective for the stimulation of the immune system because AEPB contains a large number of proteins and polysaccharides (Yoon et al., 2020). Furthermore, the immunostimulating effects of AEPB will be evaluated using in *vivo* animal models.

1.5 Conclusions

We found that AEPB increased the expression of immunostimulants and pro-

inflammatory cytokines in RAW 264.7 macrophages through activation of the TLR4-mediated NF-κB signaling pathway. Therefore, AEPB may be a promising therapeutic and nutritional agent for the treatment of immunodeficiency disorders and cancers.

Chapter 2

An Aqueous Extract of Freeze-dried *P. brevitarsis* Larvae Promotes Osteogenic Gene Expression and Bone Formation by Activating β-Catenin

Abstract

White-spotted flower chafer (*Protaetia brevitarsis*) larvae are edible insect with plenty of nutrients and minerals and possess neuroprotective and antioxidative activity. However, whether aqueous extract of *P. brevitarsis* (AEPB) influences on osteogenesis has not been elucidated. In this study, we found that AEPB highly promotes expression of osteogenic genes including runt-related transcription factor 2 (RUNX2), osterix (OSX), and alkaline phosphatase (ALP) along with high level of mineralization in preosteoblast MC3T3-E1 cells. Moreover, AEPB accelerated vertebral formation in zebrafish larvae accompanied by the osteogenic gene expression. Inhibition of the Wnt/β-catenin signaling pathway using FH535 suppressed AEPB-induced osteogenic gene expression and vertebral formation, which indicates that AEPB stimulated osteogenesis by activating the Wnt/β-catenin signaling pathway. Taken together, this study confirms that AEPB is a promising supplement for osteoblast differentiation and bone formation. Nevertheless, whether AEPB inhibits bone resorption diseases such as osteoporosis should be evaluated in higher animal models.

Keywords: *Protaetia brevitarsis*; Osteoblast differentiation; Bone formation; β-catenin

2.1 Introduction

Bone is a highly dynamic organ system that maintains homeostasis through the balance between bone-forming osteoblasts and bone-resorbing osteoclasts (Chen et al., 2018). Disruption of the balance abnormally impairs bone architecture or function and leads to bone metabolic diseases such as osteoporosis or osteopetrosis (Chen et al., 2018; Kim et al., 2020). Recently, many studies have demonstrated that the incidence rate of osteoporosis has been increasing in elderly men and postmenopausal women with low bone mass, resulting from the inactivation of osteoblasts and activation of osteoclasts (Sozen et al., 2017; Tian et al., 2017). Mahmoud et al. (Mahmoud et al., 2020) reported that osteoblast-based therapy is a promising strategy for the treatment of osteoporosis through bone remodeling. Therefore, a potential bone-forming platform, which results in an increase in bone density and integrity, would be a great avenue and solution against bone-resorbing diseases such as osteoporosis (Ling et al., 2017).

Osteogenesis is a multiple process of osteoblast development that involves the formation of new bone material through the activation of many transcription factors such as Wnt/β-catenin, runt-related transcription factor 2 (RUNX2), and osterix (OSX), accompanied by mineralization (Felber et al., 2015). At the early development stage, the Wnt/β-catenin pathway promotes the differentiation of bone marrow-derived mesenchymal stem cells (BM-MSCs) to osteoprogenitors, and the activation is maintained in mature osteoblasts accompanied by mineralization. However, the differentiation capacity of the pathway significantly decreases in osteoporosis, resulting in a reduction of bone formation, which indicates that the Wnt/β-catenin pathway regulates early differentiation from BM-MSCs to preosteoblasts (Hu et al., 2018) as

well as complete differentiation to mature osteoblasts. In addition, Wnt/β-catenin canonically activates RUNX2 and OSX, which stimulates the differentiation of preosteoblasts from BM-MSCs (Felber et al., 2015; Gaur et al., 2005). Alkaline phosphatase (ALP) is also one of the key regulating enzymes in differentiation to fully mature osteoblasts, and a significant increase in ALP activity in the tissue or cells represents potential evidence of mature osteoblasts and mineralization (Trivedi et al., 2020). More specifically, ALP catalyzes the hydroxylation of inorganic pyrophosphate (PPi) to generate inorganic phosphate (Pi), confirming the balance between PPi and Pi concentrations in the mineralization process (Orimo, 2010). Many phytochemical compounds have been developed as bioactive strategies for bone tissue regeneration by activating osteoblast differentiation (Valentino et al., 2021).

Nutrient supplements derived from insects or their derivatives are known to be good sources of proteins, fatty acids, minerals, and vitamins (Oonincx and Finke, 2021). More than 2,000 species of insects are consumed in the world as edible and dietary supplements with nutrients comparable to other meat sources (Tao and Li, 2018). In particular, *Protaetia brevitarsis* larvae are considered promising sources for the treatment of many human diseases, such as stomatitis, tetanus, hepatic cancer, liver cirrhosis, and cerebral stroke in Korean traditional medicine (Ham et al., 2021). Recently, scientists reported that freeze-dried *P. brevitarsis* larva contained 58% crude protein, 17% crude fat, and 11% total carbohydrate with crude ash and fiber, and showed no evidence of mutagenic and carcinogenic potential in te genotoxic studies (Noh et al., 2018; Yoon et al., 2020). Additionally, the extract of *P. brevitarsis* larvae possessed antioxidant and anticancer activities (Suh and Kang, 2012; Yoo et al., 2007). In a recent study, we demonstrated that an aqueous extract of freeze-dried *P. brevitarsis* larvae (AEPB) stimulates the immune response in RAW 264.7 macrophages by activating the NF-κB signaling pathway (Jayasingha et al., 2021). However, whether AEPB promotes osteoblast

differentiation and bone formation has not been evaluated.

In the present study, we investigated whether AEPB promotes the differentiation of preosteoblast MC3T3-E1 cells and enhances bone mineralization and formation in zebrafish larvae. We found that AEPB significantly stimulated osteogenesis both in vitro and in vivo, indicating that AEPB could be used as a functional supplement to increase bone mass and density.

2.2 Materials and Methods

2.2.1 Preparation of AEPB

Freeze-dried P. brevitarsis larva powder was supplied from Huimang-Gonchung Farm (2626-11 Gajogaya-ro, Gaya-myeon, Hapcheongun, Gyeongsangnamdo, Republic of Korea). The specimens were authenticated and deposited at Nakdonggang National Institute of Biological Resources (Sangju, Gyeongsangbukdo, Republic of Korea). To obtain AEPB, approximately 100 g of the powder was extracted with 1 L of water for 1 h. The solids and water were removed by vacuum filtration and freeze drying. Total yield was approximately 23%.

2.2.2 Reagents and antibodies

Alizarin red, calcein, β-glycerophosphate (GP), and FH535 were purchased from Sigma-Aldrich Chemical Co. (St. Louis, MO, USA). Specific antibodies against RUNX2, ALP, OSX, β-actin, and nucleolin were purchased from Santa Cruz Biotechnology (Santa Cruz, CA, USA). All other chemicals were supplied from Sigma-Aldrich Chemical Co. Minimum Essential Medium Alpha Modification (α-MEM), fetal bovine serum (FBS), and antibiotics mixture were obtained from WelGENE (Gyeongsan, Gyeongsangbukdo, Republic of Korea).

2.2.3 Cell culture and Flow cytometry

Mouse preosteoblast MC3T3-E1 cells were obtained by the American Type Culture Collection (ATCC, Manassas, VA, USA) and maintained in α-MEM supplemented with 10% FBS and antibiotics mixture in a humidified incubator at 5% CO_2 and 37℃. In order to determine viable and dead cell population, MC3T3-E1 cells were seeded into 24-well plates at a density of 1×10^4 cells/mL and incubated with different concentrations (0–40 μg/mL) of AEPB for 12 days. Fresh media were replenished with AEPB every 3 days. Hydrogen peroxide (H_2O_2, 300 mM) was used as a positive control for inducing cell death and treated for last 24 h. Then, the cells were stained using a Cell Count & Viability Kit (Luminex, Austin, TX, USA) for 5 min and analyzed using a Muse Cell Analyzer (Luminex).

2.2.4 Alizarin red staining

MC3T3-E1 cells were seeded in a 24-well plate at a density of 1×10^4 cells/mL and then incubated for 12 days after treatment with different concentrations of AEPB (0–20 μg/mL). Fresh media were replenished with AEPB every 3 days. In vitro calcium deposition was measured by staining with 2% alizarin red. Briefly, MC3T3-E1 cells were washed with 1X phosphate-buffered saline (PBS) and fixed with 4% paraformaldehyde for 30 min at 37℃. Then, the cells were stained with 2% alizarin red solution for 30 min, and images of each well were taken using a phase contrast microscope (Ezscope i900PH, Macrotech; Goyang, Gyeonggi-do, Republic of Korea).

2.2.5 Alkaline phosphatase (ALP) activity

MC3T3-E1 cells were seeded in 24-well plates and then treated with the different concentrations of AEPB (0–20 μg/mL) for 12 days. The media were freshly replaced with AEPB every 3 days. GP was used as a positive control for inducing osteoblast differentiation.

ALP activity was measured using a tartrate-resistant acid phosphatase (TRACP) & ALP double-stain Kit (Takara Bio Inc., Kusatsu, Shiga, Japan) according to the manufacture's protocol. Briefly, the cells were rinsed three times with PBS and incubated with the fixation buffer for 5 min. Then, ALP substrate was added into each well and incubated at 37℃ for 45 min. The images of each well were taken using a phase contrast microscope (Ezscope i900PH).

2.2.6 Reverse transcription-polymerase chain reaction (RT-PCR)

MC3T3-E1 cells were treated with the different concentrations of AEPB for the indicated days, and total RNA was extracted using easy-BLUE Total RNA Extraction Kit (iNtRON Biotechnology, Sungnam-si, Gyeonggi-do, Republic of Korea) according to the manufacturer's instruction. Two micrograms of RNA were reverse-transcribed using MMLV reverse transcriptase (Bioneer, Daejeon, Republic of Korea). The target genes were amplified using the specific primers (Molagoda et al., 2019); *mRUNX2* with 171 bp at 60℃ (forward: 5′ -CAT GGT GGA GAT CAT CGC GG-3′, and reverse: 5′-GGC CAT GAC GGT AAC CAC AG-3′), *mALP* with 198 bp at 60ºC (forward 5′-TTG TGG CCC TCT CCA AGA CA-3′ and reverse 5′-GAC TTC CCA GCA TCC TTG GC-3′), *mOSX* with 194 bp at 60℃ (forward 5′-AAG GCG GTT GGC AAT AGT GG-3′ and reverse 5′-GCA GCT GTG AAT GGG CTT CT-3′) and *mGAPDH* with (forward 5′-ACC ACA GTC CAT GCC ATC AC -3′ and reverse 5′-CAC CAC CCT GTT GCT GTA GC-3′). In a zebrafish model, cDNA was synthesized and amplified using the zebrafish primers (Chen et al., 2017); *zRUNX2a* with 173 bp at 58℃ (forward 5′-GAC GGT GGT GAC GGT AAT GG-3′ and reverse 5′-TGC GGT GGG TTC GTG AAT A-3′), *zOSX* with 153 bp at 56℃ (forward 5′-GGCTATGCTAACTGCGACCTG-3′ and reverse 5′-GCT TTC ATT GCG TCC GTT TT-3′), and *zALP* with149 bp at 44℃ (5′-CAA GAA CTC AAC AAG AAC-3′ and reverse 5′-TGA GCA TTG GTG TTA TAC -3′), *zβ-actin* with 154

bp at 61℃ (forward 5′-CGA GCG TGG CTA CAG CTT CA-3′ and reverse 5′-GAC CGT CAG GCA GCT CAT AG-3′).

2.2.7 Protein extraction and western blotting

MC3T3-E1 cells (1×10^4 cells/mL) were harvested and lysed with RIPA lysis buffer (iNtRON biotechnology) with protease inhibitors (Sigma). Then, proteins were collected and quantified using a Bio-Rad Protein Assay Reagents (Bio-Rad, Hercules, CA, USA). In a parallel experiment, nuclear proteins were extracted using NE-PER Nuclear and Cytoplasmic Extraction Reagents (Pierce, Rockford, IL, USA). An equal amount of protein was separated by sodium dodecyl sulfate (SDS)-polyacrylamide gel, transferred onto nitrocellulose membrane (Schleicher & Schuell, Keene, NH, USA) and then immunoblotted with specific antibodies.

2.2.8 Bone mineralization in zebrafish larvae

Zebrafish was raised and handled according to standard guidelines of the Animal Care and Use Committee of Jeju National University (Jeju Special Self-Governing Province, Republic of Korea; approval No.: 2021-0065). All experiments were carried out in accordance with the approved guidelines (Percie du Sert et al., 2020). For evaluating vertebral formation in zebrafish larvae, calcein green was used. To visualize vertebrae, zebrafish larvae at (*n=20* in each group) at 3 days post-fertilization (dpf) were treated with 0–200 μg/mL AEPB by 12 dpf. GP (4 mM) was used as a positive control for stimulating vertebral formation in zebrafish. The E3 culture media (5 mM NaCl, 0.17 mM KCl, 0.33 mM $CaCl_2$, 0.33 mM $MgSO_4$) containing 2 mg/L methylene blue was changed every 3 days. At 12 dpf, the larvae were immersed in 0.05% calcein solution for 10 min and then rinsed in fresh water three times for 10 min in order to allow diffusion of the free calcein. After rinsing, the larvae were anesthetized

in 0.03 % tricaine methanesulfonate solution and mounted on depression slides using 2% methylcellulose before imaging. In a parallel experiment, zebrafish larvae at 3 dpf were treated with 10 μM FH535 for 24 h prior to treatment with AEPB (200 μg/mL) to evaluate the Wnt/β-catenin pathway in bone mineralization.

2.2.9 Statistical analysis

The images of RT-PCR and western blotting were visualized by ImageQuant LAS 500 (GE Healthcare Bio-Sciences AB, Uppsala, Sweden). Statistical analysis was performed and graphed using Sigma Plot 12.0 software (Systat Software, San Jose, CA, USA, www.systatsoftware.com) by unpaired one-way analysis of variance (ANOVA) with Bonferroni correction. All data were expressed as the mean ± the standard error of the median (SEM). Statistical significance was set at ***, $p < 0.001$.

2.3 Results

2.3.1 No cytotoxicity in preosteoblast MC3T3-E1 cells was shown at low concentrations of AEPB

No significant toxicity was observed in MC3T3-E1 cells (Figure 1A). As shown in Figure 1B, the viable cell populations were (88.37 ± 0.15) %, (88.47 ± 0.42) %, (85.17 ± 0.27) %, and (82.94 ± 0.67) % at the concentrations of 5, 10, 20, and 40 μg/mL AEPB, respectively, compared with that in the untreated cells (88.93 ± 0.67) %. However, H_2O_2 treatment significantly decreased cell viability (52.53 ± 3.76) %. In addition, no significant increase in dead cell populations was observed in the presence of AEPB (11.63 ± 0.67) %, (11.53 ± 0.27) %, and (17.06 ± 0.67) % at 5, 10, 20, and 40 μg/mL, respectively compared with that in the untreated cells (11.07 ± 0.67) %; however, H_2O_2 significantly increased the dead cell

population (47.47 ± 3.77) % (Figure 1C). These results indicate that low concentrations of AEPB did not induce toxicity in MC3T3-E1 cells; however, 40 μg/mL AEPB increased morphological irregularity with many small vacuoles in the cells (data not shown). Therefore, AEPB at concentrations below 20 μg/mL were used for further experiments. Viable and dead cell populations were determined by flow cytometry. *** $p < 0.001$ vs. untreated cells.

2.3.2 AEPB promotes ALP activity and calcium deposition in preosteoblast MC3T3-E1 cells

To address whether AEPB induces full mature osteoblast from preosteoblast MC3T3-E1 cells, ALP activity and mineralization were investigated. As shown in Figure 7A, 5 μg/mL AEPB moderately increased ALP activity compared with that in the untreated cells, and over 20 μg/mL remarkably stimulated ALP activation. Bone-stimulating agent, GP, more significantly upregulated ALP activity. The data indicates that AEPB induces full maturation of osteoblast. Furthermore, to evaluated whether AEPB increases Ca^{2+} deposition in MC3T3-E1 cells, alizarin red staining was performed on day 12. Consistent with the data of ALP activity, AEPB markedly increased Ca^{2+} deposition comparable to that in the cells treated with GP (Figure 7B), suggesting that AEPB enhances calcification in MCT3C-E1 cells. Taken together, the data indicate that AEPB stimulates full maturation of osteoblast, leading to the calcification.

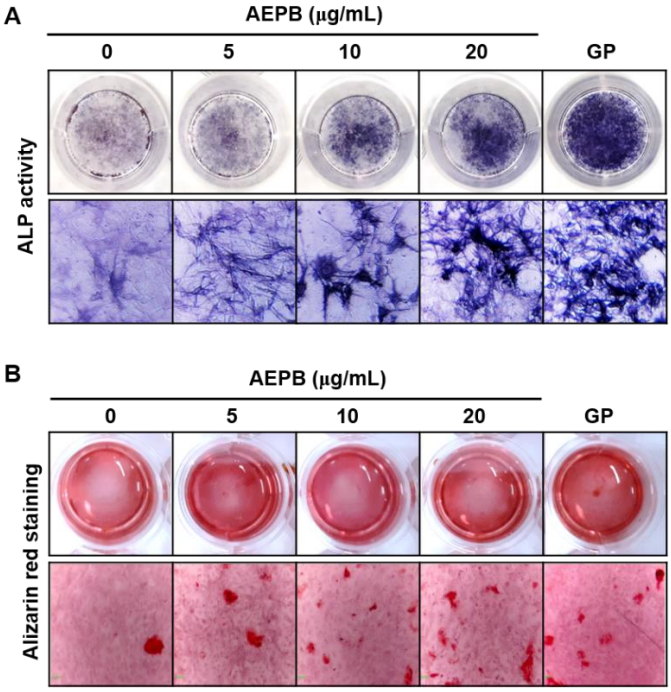

Figure 6. An aqueous extract of freeze- dried *Protaetia brevitarsis* larvae (AEPB) promotes osteoblast differentiation and calcification.

MC3T3-E1 cells (1× 10^4 cells/mL) were treated with APEB (0–20 μg/mL) for 12 days. β-Glycerophosphate (GP, 2 mM) was used as the bone-stimulating positive control. ALP activity was detected using a TRACP & ALP Double Staining Assay Kit (A). Calcification in MC3T3-E1 cells was measured using 2 % alizarin red (B). The images were captured using phase contrast microscopy (× 10).

2.3.3 AEPB enhances expression of osteogenic markers including RUNX2, OSX, and ALP

To confirm whether AEPB increases expression of osteogenic makers including RUNX2, OSX, and ALP, RT-PCR and western blotting were performed 12 days after AEBP treatment. As expected, AEPB upregulated all genes tested in this study including *RUNX2*, *OSX*, and *ALP* in a dose-dependent manner, and the highest concentration of AEPB increased the expression comparable to that in GP-treated cells (Figure 8A). Consistent with RT-PCR data, all tested proteins gradually increased in MC3T3-E1 cells (Figure 8B). The data indicate that

AEPB is an activator of osteogenic markers including RUNX2, OSX, and ALP.

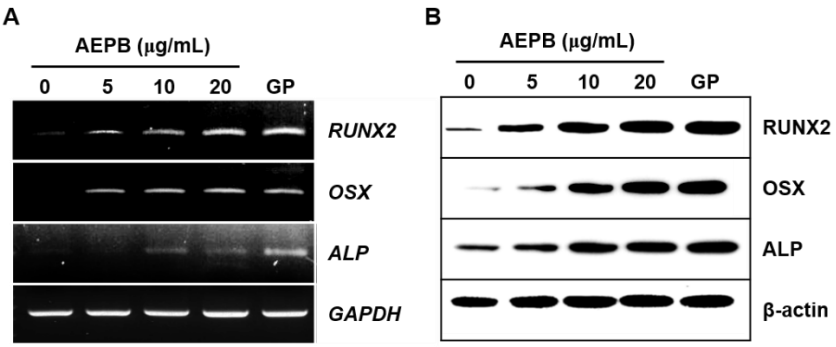

Figure 7. An aqueous extract of freeze- dried *Protaetia brevitarsis* larvae (AEPB) promotes expression of osteogenic markers including runt-related transcription factor 2 (RUNX2), osterix (OSX), and alkaline phosphatase (ALP) in preosteoblast MC3T3-E1 cells.

MC3T3-E1 cells (1×10^4 cells/mL) were treated with the indicated concentrations of APEB (0–20 μg/mL) or β-glycerophosphate (GP, 2 mM) for 12 days. (A) Total RNA was extracted by easy-BLUE Total RNA Extraction Kit, and RT-PCR was performed to determine the expression of *RUNX2*, *OSX*, and *ALP*, and *GAPDH* was as the internal control. The total protein was extracted using RIPA lysis buffer with protease inhibitors, and western blotting was performed using specific antibodies against RUNX2, OSX, and ALP. β-Actin was used as the internal control. β-Glycerophosphate (GP, 2 mM) was used as the gene-stimulating positive control.

2.3.4 AEPB promotes bone formation in zebrafish larvae accompanied by high expression of osteogenic genes including RUNX2a, OSX, and ALP

Next, we investigated whether AEPB promotes osteogenic gene expression and bone formation in zebrafish larvae. The data based on calcein staining showed that AEPB accelerates vertebral formation in a dose-dependent manner (Figure 9A). GP also markedly increased vertebral formation. Median vertebral numbers significantly ascended in zebrafish larvae treated with 100 μg/mL AEPB (6.33 ± 0.33) compared with that in the untreated larvae (3.33

± 0.33), and reached at 7.33 ± 0.33 in 200 μg/mL AEPB-treated larvae (Figure 9B). Vertebra-forming ability of GP was the strongest (9.33 ± 0.33). However, 50 μg/mL AEPB slightly increased vertebral formation (5.33 ± 3.33), but significant in statistical analysis. Additionally, we evaluated osteogenic gene expression in zebrafish larvae at 12 dpf after AEPB treatment. As expected, all genes including *RUNX2a*, *OSX*, and *ALP* were activated in a dose-dependent manner, when AEPB and GP were treated (Figure 9C). The data indicate that AEPB is a bone-stimulating candidate by activating the expression of osteogenic genes.

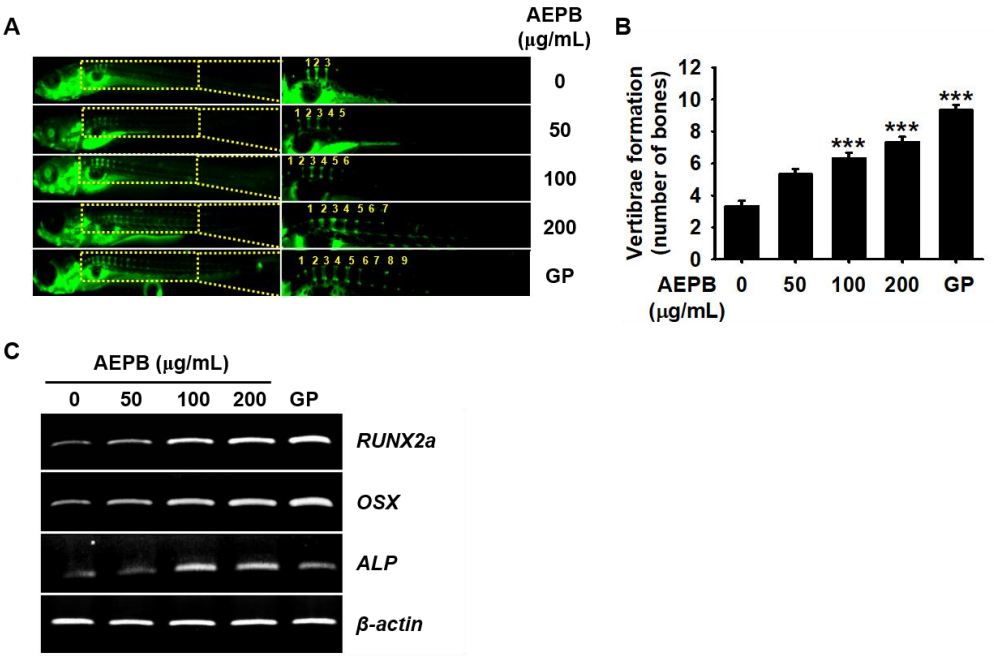

Figure 8. An aqueous extract of freeze-dried *Protaetia brevitarsis* larvae (AEPB) stimulates vertebral formation in zebrafish larvae accompanied by high levels of osteoblast differentiation marker genes including runt-related transcription factor 2 (RUNX2), (OSX), and alkaline phosphatase (ALP).

(A) Zebrafish larvae (*n=20*) at 3 days post-fertilization (dpf) were treated with the indicated concentration of AEPB (0–200 μg/mL) and 4 mM β-glycerophosphate (GP) and stained with 0.05% calcein to visualize vertebral formation at 12 dpf. (B) The number of vertebrae manually was counted. (C) Total RNA was extracted from zebrafish larvae at 12 dpf, and RT-PCR was

performed to determine expression of *RUNX2a*, *OSX*, and *ALP. β-Actin* was used as the internal. *** $p < 0.001$ vs. untreated zebrafish larvae.

2.3.5 AEPB promotes osteoblast differentiation and bone formation by activating the Wnt/β-catenin pathway

Since the Wnt/β-catenin signaling pathway is considered one of major mechanism in osteogenesis from BM-MSC to mature osteoblast throughout (Gaur et al., 2005; Hu et al., 2018), we evaluated the significance of the Wnt/β-catenin signaling pathway using an Wnt/β-catenin inhibitor, FH535. RT-PCR data showed that FH535 markedly downregulated AEPB-induced high expression of osteogenic genes including *RUNX2*, *OSX*, and *ALP* in MC3T3-E1 cells (Figure 10A). In the western blotting result, we found that FH535 strongly inhibited AEPB-induced nuclear β-catenin in MC3T3-E1 cells (Figure 10B). Furthermore, calcein-stained zebrafish larvae showed that FH535 markedly reduced AEPB-induced vertebral formation (Figure 10C). Untreated and FH535-treated larvae only showed lower number of vertebrae than AEPB treatment. In particular, the quantitative number of vertebrae in zebrafish larvae showed that AEPB-induced vertebral number was significantly reduced in the presence of FH535 from 7.33 ± 0.33 to 3.67 ± 0.33 (Figure 10D). Vertebral number in untreated and FH535-treated larvae was almost similar levels, 3.00 ± 0.58 and 2.00 ± 0.33, respectively. Consistent with vertebral formation, RT-PCR results showed that AEPB activated expression of *RUNX2a*, *OSX*, and *ALP*, and FH535 reduced the expression (Figure 10E). Above data indicate that AEPB-induced osteogenic gene expression and vertebral formation are regulated by activating the Wnt/β-catenin signaling pathway.

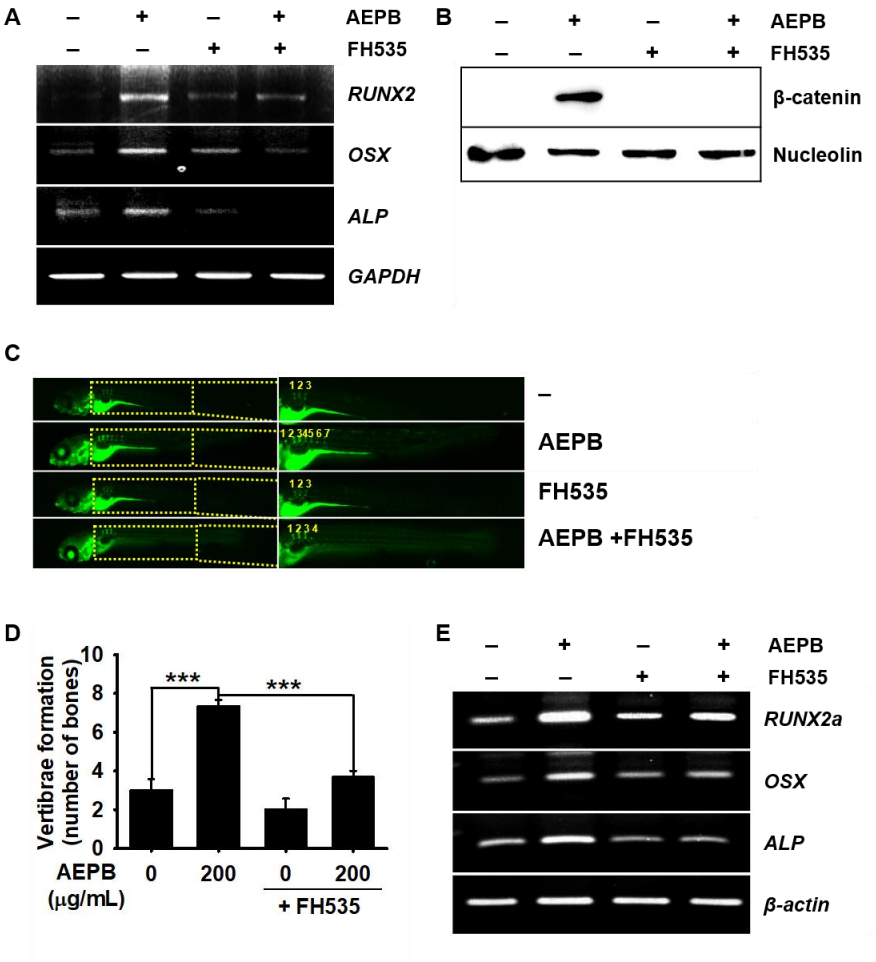

Figure 9. An aqueous extract of freeze-dried *Protaetia brevitarsis* larvae (AEPB) promotes osteogenic gene expression and vertebral formation through the Wnt/β-catenin signaling pathway.

MC3T3-E1 cells (1×10^4 cells/mL) were treated with 20 μg/mL APEB in the presence and absence of 10 μM FH535 for 12 days. (A) Total RNA was extracted and RT-PCR was performed to evaluate expression of runt-related transcription factor 2 (*RUNX2*), osterix (*OSX*), and alkaline phosphatase (*ALP*). Glyceraldehyde 3-phophate dehydrogenase (*GAPDH*) was used as the internal control. (B) Nuclear protein was extracted using a NE-PER Nuclear Protein Extraction Kit, and western blotting was performed to determine the expression β-catenin. β-Actin was used as the internal control. (C) Zebrafish larvae at 3 days post-fertilization (dpf) were treated with 10 μM FH535 24 h before treatment with 200 μg/mL AEPB. The zebrafish

larvae at 12 dpf were stained with 0.05% calcein to visualize vertebral formation. (D) The number of vertebrae was counted manually. *** $p < 0.001$. (E) In a parallel experiment, RNA was extract from zebrafish larvae at 12 dpf, and RT-PCR was performed to detect expression of *RUNX2a*, *OSX*, and *ALP*.

2.4 Discussion

Osteoporosis is a skeletal disorder and characterized by increasing bone resorption accompanied by loss of bone mass and bone mineral density via inactivation of osteoblast and overactivation of osteoclast (Compston et al., 2019). As the elderly population is increasing in the worldwide, osteoporotic patients are steadily increasing, and the prevention and management of osteoporosis have been a social issue. Hence, many scientists have attempted to discover natural compounds and nutrients for osteoblast activation (Bellavia et al., 2021; Rizzoli et al., 2021). In the present study, we evaluated the potential of AEPB on osteoblast differentiation and bone formation because it has not known whether AEPB regulates osteogenesis, even though *P. brevitarsis* has been used as edible insects and traditional remedy with plenty of nutrients (Ham et al., 2021; Jayasingha et al., 2021; Suh and Kang, 2012; Yoon et al., 2020). In this study, we found that AEPB promotes osteoblast differentiation and bone formation by activating Wnt/β-catenin signaling pathway.

The osteoblast differentiation is characterized by the timely expressed transcription factors such as RUNX2, OSX, and ALP prior to formation of extracellular matrix (ECM) synthesis and mineralization (Dieudonne et al., 2013). In particular, RUNX2 is a master key factor for osteoblast differentiation, ECM production, and mineralization by stimulating major bone matrix component genes (Komori, 2017; Qin et al., 2021). In previous, *RUNX2*-deficient mice completely inhibited *OSX* expression along with loss of ALP activity and mineralization

(Nakashima et al., 2002), whereas RUNX2 was normally expressed in OSX-deficient (Komori, 2019), indicating that RUNX2 is an upstream molecule of OSX in osteoblast differentiation. As a downstream transcription factor of RUNX2, OSX is specifically expressed from preosteoblast to mature osteoblast, and *OSX*-null embryos failed to bone formation (Nakashima et al., 2002). In the present study, we found that AEPB promotes osteoblast differentiation characterized by high levels of RUNX2, OSX, and ALP concomitant with mineralization in MC3T3-E1 cells and vertebral formation in zebrafish. The data show the potential of AEPB as an osteogenic supplement. Nevertheless, Shrivats et al. (Shrivats et al., 2015) demonstrated that *RUNX2* and *OSX* siRNA delivery significantly reduced mineralization in osteoblast cells accompanied by inhibition of ALP activity, but completely eliminated, which indicates that osteogenesis complicatedly regulated. Therefore, the detail effect of AEPB at each stage of osteoblast development should be evaluated.

The Wnt/β-catenin signaling pathway is known to promote preosteoblast differentiation from BM-MSC and subsequently regulate maturation and terminal differentiation of osteoblast (Hu et al., 2018). The canonical Wnt signaling pathway inhibits ubiquitination and degradation of β-catenin and promotes release of β-catenin from glycogen synthase-3β (GSK-3β) (Houschyar et al., 2018). Free β-catenin transits to the nucleus and binds to the N-terminal domain of TCF/LEF transcription factor, which transactivates key osteoblastic genes such as *RUNX2* and *OSX* (Li et al., 2018). In this study, we found that AEPB increased expression of osteogenic genes including RUNX2, OSX, and ALP, and activated nuclear translocation of β-catenin in preosteoblast MC3T3-E1 cells; however, an inhibitor of Wnt/β-catenin, FH535, inhibited the AEPB-induced activation. Furthermore, FH535 reduced AEPB-stimulated vertebral formation and osteogenic gene expression in zebrafish larvae, which indicates that AEPB-stimulated osteogenesis is positively regulated by activating the

Wnt/β-catenin signaling pathway. Nevertheless, FH535 cannot completely inhibit AEPB-induced osteogenic gene expression and vertebral formation, which suggests that other osteogenic transcription factors are also related to AEPB-induced osteogenesis. Apart from Wnt/β-catenin, there are many transcription factors such as bone morphogenic proteins (BMPs) and insulin-like growth factor (IGF) involved in osteogenesis (Plotkin and Bruzzaniti, 2019), although β-catenin is identified as one major mediator in AEPB-induced osteogenesis. Therefore, during osteogenesis, whether AEPB regulated other transcription factors should be investigated.

2.5 Conclusions

We found that AEPB promoted osteoblast differentiation MC3T3-E1 cells and vertebral formation in zebrafish larvae accompanied by high levels of osteogenic mark expression by activating the Wnt/β-catenin signaling pathway. Though we found AEPB-induced osteogenic activity, we need further study to support a potential therapeutic supplement in bone diseases such as osteoporosis.

Bibilography

Ahn, E. M., Myung, N. Y., Jung, H. A., & Kim, S. J. (2019). The ameliorative effect of *Protaetia brevitarsis* Larvae in HFD-induced obese mice. *Food Science and Biotechnology, 28*(4), 1177-1186. doi: 10.1007/s10068-018-00553-w.

Billack, B. (2006). Macrophage activation: role of toll-like receptors, nitric oxide, and nuclear factor kappa B. *American Journal of Pharmaceutical Education, 70*(5), 102. doi: 10.5688/aj7005102.

Brubaker, S. W., Bonham, K. S., Zanoni, I., & Kagan, J. C. (2015). Innate immune pattern recognition: a cell biological perspective. *Annuual Review of Immunology, 33*, 257-290. doi: 10.1146/annurev-immunol-032414-112240.

Chaplin, D. D. (2010). Overview of the immune response. *Journal of Allergy and Clinical Immunology, 125*(2 Suppl 2), S3-23. doi: 10.1016/j.jaci.2009.12.980.

Dorrington, M. G., & Fraser, I. D. C. (2019). NF-κB signaling in macrophages: Dynamics, crosstalk, and signal integration. *Frontiers in Immunology, 10*, 705. doi: 10.3389/fimmu.2019.00705.

Feng, Y., Mu, R., Wang, Z., Xing, P., Zhang, J., Dong, L., & Wang, C. (2019). A toll-like receptor agonist mimicking microbial signal to generate tumor-suppressive macrophages. *Nature Communications, 10*(1), 2272. doi: 10.1038/s41467-019-10354-2.

Gao, Y., Zhou, S., Jiang, W., Huang, M., & Dai, X. (2003). Effects of ganopoly (a *Ganoderma lucidum* polysaccharide extract) on the immune functions in advanced-stage cancer patients. *Immunological Investigations, 32*(3), 201-215. doi: 10.1081/imm-120022979.

Grassin-Delyle, S., Abrial, C., Salvator, H., Brollo, M., Naline, E., & Devillier, P. (2020).

The role of Toll-like receptors in the production of cytokines by human lung macrophages. *Journal of Innate Immunity, 12*(1), 63-73. doi: 10.1159/000494463.

Hirayama, D., Iida, T., & Nakase, H. (2017). The phagocytic function of macrophage-enforcing innate immunity and tissue homeostasis. *Int J Mol Sci, 19*(1). doi: 10.3390/ijms19010092.

Im, A. R., Yang, W. K., Park, Y. C., Kim, S. H., & Chae, S. (2018). Hepatoprotective effects of insect extracts in an animal model of nonalcoholic fatty liver disease. *Nutrients, 10*(6). doi: 10.3390/nu10060735.

Ireton, G. C., & Reed, S. G. (2013). Adjuvants containing natural and synthetic Toll-like receptor 4 ligands. *Expert Review of Vaccines, 12*(7), 793-807. doi: 10.1586/14760584.2013.811204.

Iwasaki, A., & Medzhitov, R. (2015). Control of adaptive immunity by the innate immune system. *Nature Immunology, 16*(4), 343-353. doi: 10.1038/ni.3123.

Johnson, D. A. (2013). TLR4 agonists as vaccine adjuvants: a chemist's perspective. *Expert Review of Vaccines, 12*(7), 711-713. doi: 10.1586/14760584.2013.811189.

Lee, J., Hwang, I. H., Kim, J. H., Kim, M.-A., Hwang, J. S., Kim, Y. H., & Na, M. (2017). Quinoxaline-, dopamine-, and amino acid-derived metabolites from the edible insect *Protaetia brevitarsis seulensis*. *Archives of Pharmacal Research, 40*(9), 1064-1070. doi: 10.1007/s12272-017-0942-x.

Li, J., Wang, X., Wang, W., Luo, J., Aipire, A., Li, J., & Zhang, F. (2015). *Pleurotus ferulae* water extract enhances the maturation and function of murine bone marrow-derived dendritic cells through TLR4 signaling pathway. *Vaccine, 33*(16), 1923-1933. doi: 10.1016/j.vaccine.2015.02.063.

Liu, T., Zhang, L., Joo, D., & Sun, S. C. (2017). NF-κB signaling in inflammation. *Signal*

Transduction and Targeted Therapy, 2. doi: 10.1038/sigtrans.2017.23.

Locati, M., Mantovani, A., & Sica, A. (2013). Macrophage activation and polarization as an adaptive component of innate immunity. *Advances in Immunology, 120*, 163-184. doi: 10.1016/B978-0-12-417028-5.00006-5.

Molagoda, I. M. N., Choi, Y. H., Lee, S., Jin, C. Y., & Kim, G. Y. (2019). Deoxynivalenol increases the expression of pro-inflammatory genes and mediators accompanied by NF-κB activation. *Latin American Journal of Pharmacy, 38*(2), 388-395.

Noh, J. H., Jeong, J. S., Park, S. J., Yun, E. Y., Hwang, J. S., Kim, J. Y., .Jung, K. J., Park, H. J., Son, H. Y., & Moon, K. S. (2018). Toxicological safety evaluation of freeze-dried *Protaetia brevitarsis* larva powder. *Toxicology Reports, 5*, 695-703. doi: 10.1016/j.toxrep.2018.06.001.

Rahman, M. M., & McFadden, G. (2011). Modulation of NF-κB signalling by microbial pathogens. *Nature Reviews Microbiology, 9*(4), 291-306. doi: 10.1038/nrmicro2539.

Riera Romo, M., Perez-Martinez, D., & Castillo Ferrer, C. (2016). Innate immunity in vertebrates: an overview. *Immunology, 148*(2), 125-139. doi: 10.1111/imm.12597.

Suh, H. J., & Kang, S. C. (2012). Antioxidant activity of aqueous methanol extracts of *Protaetia brevitarsis* Lewis (Coleoptera: Scarabaedia) at different growth stages. *Natural Product Research, 26*(6), 510-517. doi: 10.1080/14786419.2010.530267.

Yoo, Y. C., Shin, B. H., Hong, J. H., Lee, J., Chee, H. Y., Song, K. S., & Lee, K. B. (2007). Isolation of fatty acids with anticancer activity from *Protaetia brevitarsis* larva. *Archives of Pharmacal Research, 30*(3), 361-365. doi: 10.1007/BF02977619

Yoon, C. H., Jeon, S. H., Ha, Y. J., Kim, S. W., Bang, W. Y., Bang, K. H., . . . Cho, Y. S. (2020). Functional chemical components in *Protaetia brevitarsis* Larvae: Impact of supplementary feeds. *Food Science of Animal Resources, 40*(3), 461-473. doi:

10.5851/kosfa.2020.e25.

Zhang, X., Qi, C., Guo, Y., Zhou, W., & Zhang, Y. (2016). Toll-like receptor 4-related immunostimulatory polysaccharides: Primary structure, activity relationships, and possible interaction models. *Carbohydrate Polymers, 149*, 186-206. doi: 10.1016/j.carbpol.2016.04.097. Bellavia, D., Caradonna, F., Dimarco, E., Costa, V., Carina, V., De Luca, A., Raimondi, L., Fini, M., Gentile, C., Giavaresi, G., 2021. Non-flavonoid polyphenols in osteoporosis: Preclinical evidence. Trends Endocrinol Metab 32, 515-529.

Chen, J.R., Lai, Y.H., Tsai, J.J., Hsiao, C.D., 2017. Live fluorescent staining platform for drug-screening and mechanism-analysis in zebrafish for bone mineralization. Molecules 22.

Chen, X., Wang, Z., Duan, N., Zhu, G., Schwarz, E.M., Xie, C., 2018. Osteoblast-osteoclast interactions. Connect Tissue Res 59, 99-107.

Compston, J.E., McClung, M.R., Leslie, W.D., 2019. Osteoporosis. Lancet 393, 364-376.

Dieudonne, F.X., Sévère, N., Biosse-Duplan, M., Weng, J.J., Su, Y., Marie, P.J., 2013. Promotion of osteoblast differentiation in mesenchymal cells through Cbl-mediated control of STAT5 activity. Stem Cells 31, 1340-1349.

Felber, K., Elks, P.M., Lecca, M., Roehl, H.H., 2015. Expression of osterix is regulated by FGF and Wnt/β-catenin signalling during osteoblast differentiation. PLoS One 10, e0144982.

Gaur, T., Lengner, C.J., Hovhannisyan, H., Bhat, R.A., Bodine, P.V., Komm, B.S., Javed, A., van Wijnen, A.J., Stein, J.L., Stein, G.S., Lian, J.B., 2005. Canonical WNT signaling promotes osteogenesis by directly stimulating Runx2 gene expression. J Biol Chem 280, 33132-33140.

Ham, Y.K., Kim, S.W., Song, D.H., Kim, H.W., Kim, I.S., 2021. Nutritional composition

of white-spotted flower chafer (*Protaetia brevitarsis*) larvae produced from commercial insect farms in Korea. Food Sci Anim Resour 41, 416-427.

Houschyar, K.S., Tapking, C., Borrelli, M.R., Popp, D., Duscher, D., Maan, Z.N., Chelliah, M.P., Li, J., Harati, K., Wallner, C., Rein, S., Pforringer, D., Reumuth, G., Grieb, G., Mouraret, S., Dadras, M., Wagner, J.M., Cha, J.Y., Siemers, F., Lehnhardt, M., Behr, B., 2018. Wnt pathway in bone repair and regeneration - What do we know so far. Front Cell Dev Biol 6, 170.

Hu, L., Yin, C., Zhao, F., Ali, A., Ma, J., Qian, A., 2018. Mesenchymal stem cells: Cell fate decision to osteoblast or adipocyte and application in osteoporosis treatment. Int J Mol Sci 19.

Jayasingha, A., Molagoda, I., Kyoung, T., Choi, Y.H., Chang-Hee, K., Sang-Mi, Y., Gi-Young, K., 2021. An aqueous extract of freeze-dried *Protaetia brevitarsis* larvae enhances immunostimulatory activity in RAW 264.7 macrophages by activating the NF-κB signaling pathway. LATIN AMERICAN JOURNAL OF PHARMACY 40, 1265-1272.

Kim, J.M., Lin, C., Stavre, Z., Greenblatt, M.B., Shim, J.H., 2020. Osteoblast-osteoclast communication and bone homeostasis. Cells 9.

Komori, T., 2017. Roles of Runx2 in skeletal development. Adv Exp Med Biol 962, 83-93.

Komori, T., 2019. Regulation of proliferation, differentiation and functions of osteoblasts by Runx2. Int J Mol Sci 20.

Li, Z., Xu, Z., Duan, C., Liu, W., Sun, J., Han, B., 2018. Role of TCF/LEF transcription factors in bone development and osteogenesis. Int J Med Sci 15, 1415-1422.

Ling, M., Huang, P., Islam, S., Heruth, D.P., Li, X., Zhang, L.Q., Li, D.-Y., Hu, Z., Ye, S.Q., 2017. Epigenetic regulation of Runx2 transcription and osteoblast differentiation by nicotinamide phosphoribosyltransferase. Cell & Bioscience 7, 27.

Mahmoud, N.S., Mohamed, M.R., Ali, M.A.M., Aglan, H.A., Amr, K.S., Ahmed, H.H., 2020. Osteoblast-based therapy-A new approach for bone repair in osteoporosis: Pre-clinical setting. Tissue Eng Regen Med 17, 363-373.

Molagoda, I.M.N., Karunarathne, W., Choi, Y.H., Park, E.K., Jeon, Y.J., Lee, B.J., Kang, C.H., Kim, G.Y., 2019. Fermented oyster extract promotes osteoblast differentiation by activating the Wnt/β-catenin signaling pathway, leading to bone formation. Biomolecules 9.

Nakashima, K., Zhou, X., Kunkel, G., Zhang, Z., Deng, J.M., Behringer, R.R., de Crombrugghe, B., 2002. The novel zinc finger-containing transcription factor osterix is required for osteoblast differentiation and bone formation. Cell 108, 17-29.

Noh, J.H., Jeong, J.S., Park, S.J., Yun, E.Y., Hwang, J.S., Kim, J.Y., Jung, K.J., Park, H.J., Son, H.Y., Moon, K.S., 2018. Toxicological safety evaluation of freeze-dried *Protaetia brevitarsis* larva powder. Toxicol Rep 5, 695-703.

Oonincx, D.G.A.B., Finke, M.D., 2021. Nutritional value of insects and ways to manipulate their composition. Journal of Insects as Food and Feed 7, 639-659.

Orimo, H., 2010. The mechanism of mineralization and the role of alkaline phosphatase in health and disease. Journal of Nippon Medical School 77, 4-12.

Percie du Sert, N., Hurst, V., Ahluwalia, A., Alam, S., Avey, M.T., Baker, M., Browne, W.J., Clark, A., Cuthill, I.C., Dirnagl, U., Emerson, M., Garner, P., Holgate, S.T., Howells, D.W., Karp, N.A., Lazic, S.E., Lidster, K., MacCallum, C.J., Macleod, M., Pearl, E.J., Petersen, O.H., Rawle, F., Reynolds, P., Rooney, K., Sena, E.S., Silberberg, S.D., Steckler, T., Wurbel, H., 2020. The ARRIVE guidelines 2.0: updated guidelines for reporting animal research. J Physiol 598, 3793-3801.

Plotkin, L.I., Bruzzaniti, A., 2019. Molecular signaling in bone cells: Regulation of cell

differentiation and survival. Advances in protein chemistry and structural biology 116, 237-281.

Qin, X., Jiang, Q., Komori, H., Sakane, C., Fukuyama, R., Matsuo, Y., Ito, K., Miyazaki, T., Komori, T., 2021. Runt-related transcription factor-2 (Runx2) is required for bone matrix protein gene expression in committed osteoblasts in mice. J Bone Miner Res.

Rizzoli, R., Biver, E., Brennan-Speranza, T.C., 2021. Nutritional intake and bone health. Lancet Diabetes Endocrinol 9, 606-621.

Shrivats, A.R., McDermott, M.C., Klimak, M., Averick, S.E., Pan, H., Matyjaszewski, K., Mishina, Y., Hollinger, J.O., 2015. Nanogel-mediated RNAi against Runx2 and Osx inhibits osteogenic differentiation in constitutively active BMPR1A osteoblasts. ACS Biomater Sci Eng 1, 1139-1150.

Sozen, T., Ozisik, L., Basaran, N.C., 2017. An overview and management of osteoporosis. Eur J Rheumatol 4, 46-56.

Suh, H.J., Kang, S.C., 2012. Antioxidant activity of aqueous methanol extracts of *Protaetia brevitarsis* Lewis (Coleoptera: Scarabaedia) at different growth stages. Nat Prod Res 26, 510-517.

Tao, J., Li, Y.O., 2018. Edible insects as a means to address global malnutrition and food insecurity issues. Food Quality and Safety 2, 17-26.

Tian, L., Yang, R., Wei, L., Liu, J., Yang, Y., Shao, F., Ma, W., Li, T., Wang, Y., Guo, T., 2017. Prevalence of osteoporosis and related lifestyle and metabolic factors of postmenopausal women and elderly men: A cross-sectional study in Gansu province, Northwestern of China. Medicine (Baltimore) 96, e8294.

Trivedi, S., Srivastava, K., Gupta, A., Saluja, T.S., Kumar, S., Mehrotra, D., Singh, S.K., 2020. A quantitative method to determine osteogenic differentiation aptness of scaffold.

Journal of oral biology and craniofacial research 10, 158-160.

Valentino, A., Di Cristo, F., Bosetti, M., Amaghnouje, A., Bousta, D., Conte, R., Calarco, A., 2021. Bioactivity and delivery strategies of phytochemical compounds in bone tissue regeneration. Applied Sciences-Basel 11.

Yoo, Y.C., Shin, B.H., Hong, J.H., Lee, J., Chee, H.Y., Song, K.S., Lee, K.B., 2007. Isolation of fatty acids with anticancer activity from *Protaetia brevitarsis* larva. Arch Pharm Res 30, 361-365.

Yoon, C.H., Jeon, S.H., Ha, Y.J., Kim, S.W., Bang, W.Y., Bang, K.H., Gal, S.W., Kim, I.S., Cho, Y.S., 2020. Functional chemical components in *Protaetia brevitarsis* Larvae: Impact of supplementary feeds. Food Sci Anim Resour 40, 461-473.